15th World Congress on Computational Mechanics (WCCM-XV)
8th Asian Pacific Congress on Computational Mechanics (APCOM-VIII)
Virtual Congress: 31 July – 5 August 2022
S. Koshizuka (Ed.)

EFFECTIVE RANGE OF INTEGRATED FLUIDIC ACTUATORS IN STRUCTURAL ELEMENTS

MATTHIAS J. BOSCH[1], MARKUS NITZLADER[2], TIMON BURGHARDT[1], MATTHIAS BACHMANN[1], HANSGEORG BINZ[1], LUCIO BLANDINI[2] AND MATTHIAS KREIMEYER[1]

[1] Institute for Engineering Design and Industrial Design (IKTD)
University of Stuttgart
Pfaffenwaldring 9, 70569 Stuttgart, Germany
E-mail: matthias.bosch@iktd.uni-stuttgart.de, www.iktd.uni-stuttgart.de

[2] Institute for Lightweight Structures and Conceptual Design (ILEK)
University of Stuttgart
Pfaffenwaldring 14, 70569 Stuttgart, Germany
E-mail: markus.nitzlader@ilek.uni-stuttgart.de, www.ilek.uni-stuttgart.de

Key words: Adaptivity, lightweight construction, beams, slabs, integrated actuators, simulation

Abstract. *High demand for living and working space as well as the corresponding infrastructure, caused by a growing population and increasing prosperity worldwide, leads to increased consumption of mineral resources. This is accompanied by high usage of grey energy and a high output of greenhouse gas emissions. Adaptive structures represent a promising approach for mass and resource savings. Through the interaction of actuators, sensors and control units, the structure can adapt to the external loads to reduce stresses and deformations. As a result, the building material required can be reduced. For actuators integrated into slabs, new challenges arise due to the multi-axial load transfer. In particular, the aim is to achieve the largest possible effective range of the applied moment to reduce the number of actuators required. One approach is to optimize the geometry of the force-introducing surfaces inside the structural element. This paper presents a study about the correlations of the geometric parameters using numerical simulations. This enables the pre-dimensioning of the actuator and is thus a first step in its design.*

1 INTRODUCTION

The growing population and increasing prosperity lead to high demand for living and working space as well as the corresponding infrastructure. This leads to increased consumption of mineral resources, accompanied by high usage of grey energy and a high output of greenhouse gas emissions. For example, cement production is responsible for up to 10 % of global anthropogenic CO_2 emissions [1]. In addition, the design of conventional building structures is based on relatively high loads or load combinations that rarely or even never occur. Thus, today's conventional structures are oversized for most of their lifetime.

Adaptive structures represent a promising approach for mass and resource savings. Through the interaction of actuators, sensors and control units, the structure can adapt to the external loads to reduce stresses and deformations. As a result, the building material required to enable a structure stable towards all loads can be reduced. [2]

In order to respond to a wide range of load cases, the structural element has to be manipulated locally. For structural elements subjected to bending loads, integrating actuators into their cross-section is beneficial to optimize the load transfer and thus achieve material savings. Fluidic actuators are a suitable solution due to their high energy density. The functional capability of this actuation concept has been demonstrated for beams made of concrete in various simulations and on functional samples within the subproject ‘C02’ of the Collaborative Research Centre 1244 [3, 4].

Large mass savings are achieved when the material is fully and uniformly utilized. However, the effect and influence of the integrated actuators on the surrounding structure must be known to place the actuators optimally, reducing the number of actuators needed and optimizing the shape of the force application area of the actuators. So far, extensive finite element (FE) simulations were carried out for several use cases to determine the optimal distance for actuator placement and its specific component dimensions [3]. However, the area of influence has not been analyzed so far but is necessary to design the actuator or more specifically the force application surfaces within the structure. The main objective is to formulate an analytical approach for the effective range independent of the specific component dimensions with which a rough design of the force application area and the actuator placement can be done.

This paper starts by introducing the application and fundamentals of integrated actuators (sections 2 and 3). Factors influencing the actuators' range of impact are identified and evaluated based on parameter studies using FE simulations (section 4). With these results, an analytical approach is presented, which enables an initial estimation of the geometry of the force introduction surfaces (section 5).

2 STATE OF RESEARCH ON ADAPTIVE STRUCTURES

By means of sensor-actuator systems and a control unit, adaptive structures are able to react to external influences, e.g. loads, and thus always take on an optimal state. This section presents basic principles and examples of adaptive load-bearing structures and actuators.

Initial research on adaptive load-bearing structures was carried out in the 1960s [5]. Actuation of a structure can be performed externally by means of externally mounted actuators, or internally by integrating the actuators into the structure or the structural element. Internal actuation takes place, for example, in the adaptive truss by electromagnetic linear actuators [6] or by hydraulic actuators in the demonstrator high-rise building D1244 [7]. The forces are generated and applied within the structure. In the case of external actuation, the forces are generated outside the structure. Examples are the "Stuttgarter Träger" [8] or the Smart Shell [9]. In both cases, the supports are manipulated with external actuators. A concept for adapting a beam using an external cable system with fluidic actuators is presented in [10].

In order to react to deformations in a more targeted manner, actuators can be integrated directly into the cross-section of elements subjected to bending stress, such as beams or slabs. This approach was implemented within the Collaborative Research Centre 1244 (CRC 1244) "Adaptive Skins and Structures for the Built Environment of Tomorrow" at the University of

Stuttgart. Since 2017, an interdisciplinary research group has been investigating adaptive facades and adaptive structures [11].

The actuation of beams using integrated actuators was presented in [12]. In this case, fluidic actuators are integrated into the beam in an eccentric position relative to the neutral fiber. The force thus generated by the actuator results in a bending moment due to the lever arm and its distance to the neutral fiber, which counteracts the deformation caused by an external force. Thus, the deformation is effectively reduced. This could be proven both numerically and experimentally [3, 4, 13].

3 FORCE CONDUCTION BEHAVIOUR OF INTEGRATED ACTUATORS

This section describes the influence of the integrated actuators on the surrounding structure. If a pair of forces is introduced into a structural element by an integrated actuator, the force flow closes between the two force-introducing surfaces of the actuator, as shown in Figure 1. The direction of the force flow is opposed to the direction of force introduction. A limited area of compressive stress is formed against the governing force flow before the stress is homogenized along the beam according to the St. Venant principle [14]. Maximizing this fading length to increase the impact of a single actuator reduces the number of necessary actuators. For keeping force and thus the moment constant over an even longer distance, the distance between the force-applying surfaces can be increased.

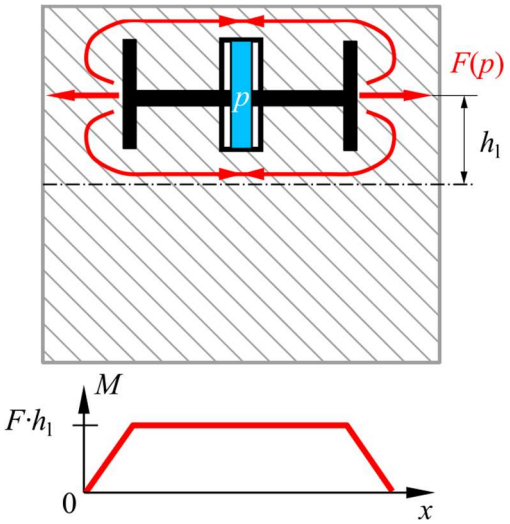

Figure 1: Force flow of an integrated actuator and induced moment curve by lever h_l

As shown in previous investigations, unidirectional force application is sufficient for the actuation principles for beams [3, 4]. In Figure 2 the schematic fading area of an actuator is shown with assumed pressure bulbs. When the stress fields of two actuators overlap, a homogeneous normal stress distribution should be achieved. Therefore, in [3] the distance between two actuators is analyzed, whereby a distance between the force application surface and the point where the normal stress reaches 50 % of the maximum value induced by a single actuator is suitable.

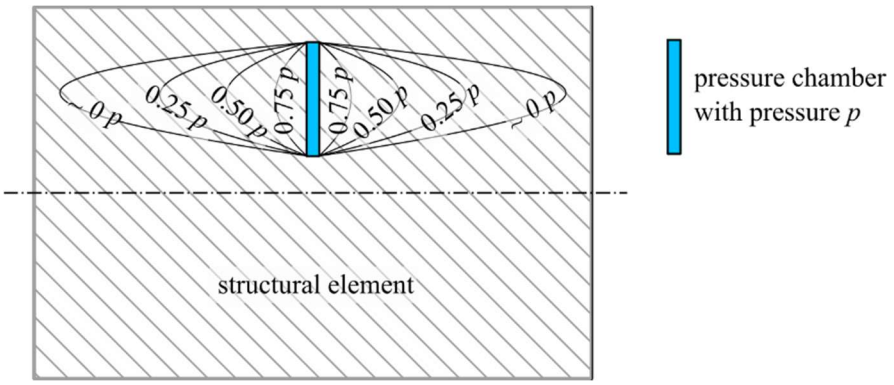

Figure 2: Schematic fading length of the pressure generated by an integrated actuator

4 NUMERICAL INVESTIGATION

The behavior of the force flow generated by an integrated actuator is analyzed by using a finite element simulation of a two-dimensional (2D) model. The influence of forces, boundary conditions, material parameters, and the geometric parameters of the force application surface were investigated. Since this study only examines the effective range of the actuator, the rough geometry presented in chapter 4.1 is sufficient. Not addressed is the determination of the precise course of the stress distribution, so the exact actuator shape is not necessary.

4.1 Geometric model

The simplified geometric structure of the actuator for the numerical investigation is shown in Figure 3. A plane state of tension is used for the 2D simulation, meaning the influence of the width of the force application surface is thus neglected, and symmetry according to Figure 3 is used (half model). The length l is chosen to be sufficiently large to avoid an influence on the effective range. This prevents overlapping of various effects and getting sharp results for different parameters. In the scope of a preliminary investigation not shown here, it was determined that a value of l greater than two times the height of the structural element is sufficient. To ensure that a value above this value is achieved, $l = 4\,h$ was chosen for the following investigation. The force application line with the size h_a was subjected to the pressure p. The resulting values were evaluated along the marked x-direction. The model was supported at the lower right corner in such a way that free movement in the x-direction is possible unless otherwise specified. The boundary conditions were part of this study. Along the symmetry planes, no movement in x-direction was possible.

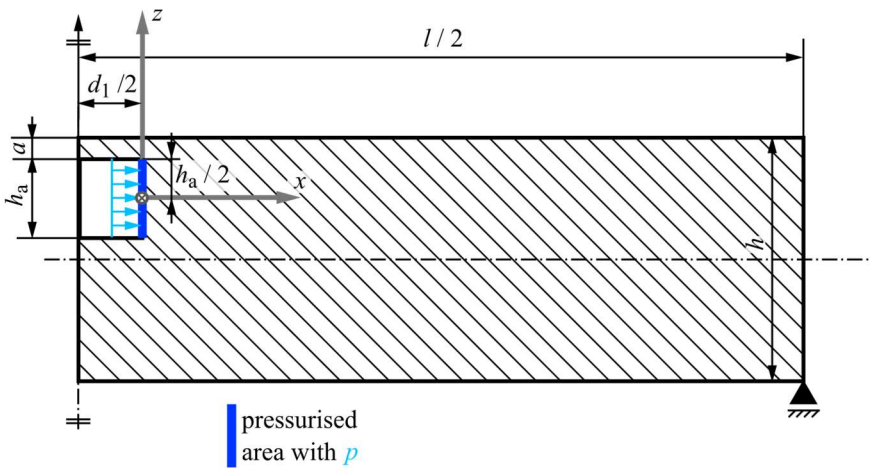

Figure 3: Geometric model and boundary conditions

For the evaluation, the geometric quantities q were normalized with the height h of the structural element to achieve more generalized results.

$$q^* = \frac{q}{h} \tag{1}$$

However, the normal stress was normalized with the maximum normal stress induced by the actuators, with the pressure value p directly at the surface.

$$\sigma^*_{\mathrm{n,x}} = \frac{|\sigma_{\mathrm{n,x}}|}{p} \tag{2}$$

Figure 4 shows the assumed independence of the stress curve from the height when normalized quantities are used.

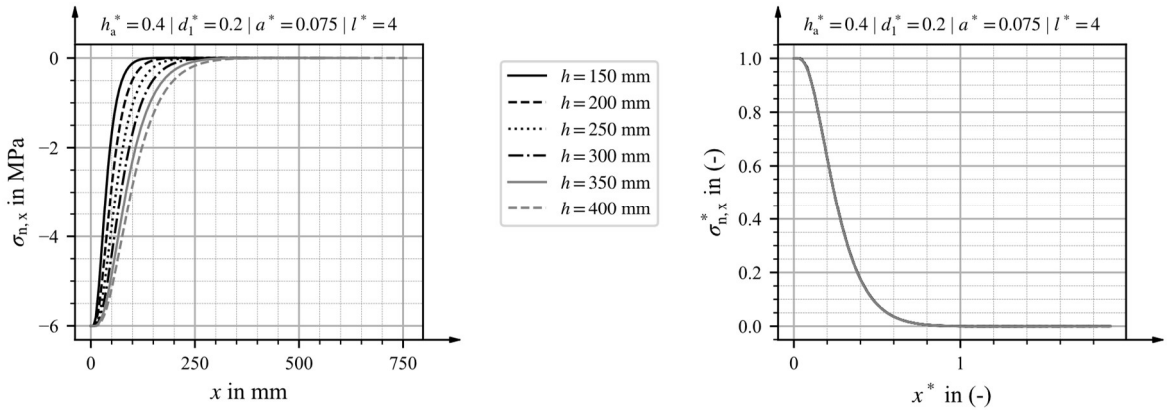

Figure 4: Influence of normalization on the values: not normalized (left) and normalized (right)

Unless otherwise specified, a height h of 200 mm is used for the following examinations. Due to the verified independence, the results can be recalculated to other values.

4.2 Mesh and material parameters

Due to the quality of the results, a quadratic element order (Quad8 elements) was chosen for meshing. The mesh is significantly refined around the force application area and around the line of evaluation marked with direction x in Figure 3, resulting in around 10,000 elements with an element size between 0.4 and 6 mm. A material with parameters in the range of concrete was used, specifically a Young's modulus of E = 30,000 MPa, a Poisson's ratio of ν = 0.18, and a density ρ = 2,300 kg/m^3. The material behavior was modeled as linear elastic.

4.3 Evaluation parameter

The distance at which the normal stress reaches 50 % of the applied pressure-induced was used to evaluate the effective range. As previously described, this value was also determined by [3] to achieve an approximately homogeneous stress distribution in the structure with a small number of actuators. With a smaller distance between two actuators, the normal stress between the actuators would be higher, which would contribute to an increased actuator effect. In Figure 5 (left) the curve for normal stress for a single actuator for different spacings between two actuators is shown. At a value of x^* = 0.14, the normal stress reaches 50 % of the induced pressure for a single actuator. This value is referred to as $x_{\sigma^*\,\mathrm{n\,x\,0.5p}}$. If the distance a_d^* between two actuators is chosen according to the considerations above with two times $x_{\sigma^*\,\mathrm{n\,x\,0.5p}}$, the first principal stress is near a maximum when superpositioning the pressure fields of two actuators (Figure 5, right). Between the actuators, the first principal stress is vertical to the structural element. For the following investigations, it is assumed that this results in a maximum upward bending moment and thus maximum effectiveness of the actuator placement. To verify this hypothesis, the exact actuation principle and the exact actuator geometries are necessary, which requires investigations beyond the scope of this study. Nevertheless, the course of the normal stress provides important information It does not drop below 80 % of the maximum induced pressure when a_d is equal to twice $x_{\sigma^*\,\mathrm{n\,x\,0.5p}}$, resulting in almost homogenous stress distribution. The chosen distance a_d is to be considered ideal. So, for the exemplary geometry given in Figure 5, the ideal distance a_d^* equals 0.28. As can be seen in Figure 5, the normal stress curve runs similarly for slightly different values of a_d^*. A larger stress drop only occurs at higher values. A slight manufacturing and assembly-related deviation in the placement of the actuators within the component should therefore not have a major impact on the effectiveness.

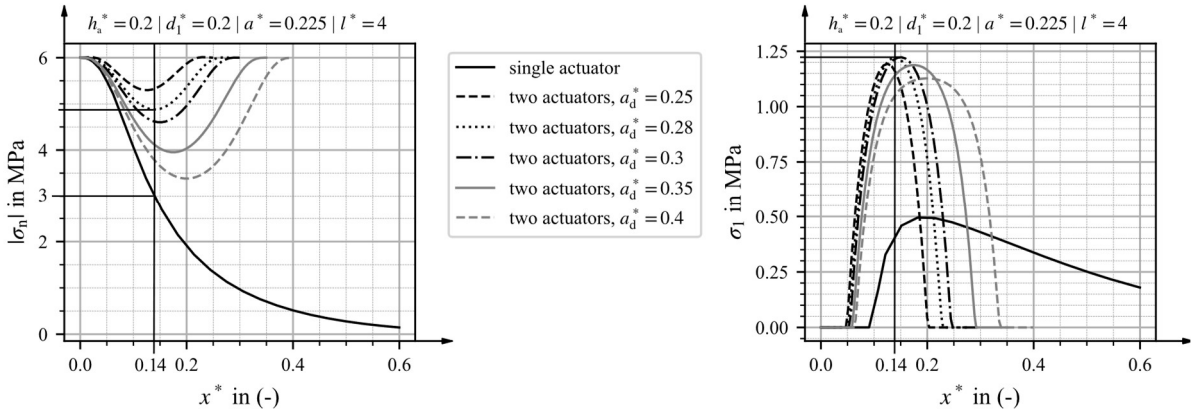

Figure 5: Normal stress in x-direction (left) and maximum principal stress (right) between two actuators for different actuator spacings a_d^*

4.4 Influence of forces and boundary conditions (BC)

Since the material model used is linearly elastic, the level of applied pressure does not influence the results for the decay length. A pressure of 60 bar was applied for the investigations, which is within the expected range for the application.

The influence of the selected boundary conditions (BC), statically determined or statically overdetermined, is shown in Figure 6 (right). The statically overdetermined state is achieved by locking the support at the right edge in the x-direction. An influence on the normal stress curve can only be observed for x^* outside the relevant area for the investigation. Therefore, the statically determined system can be selected for the following investigations.

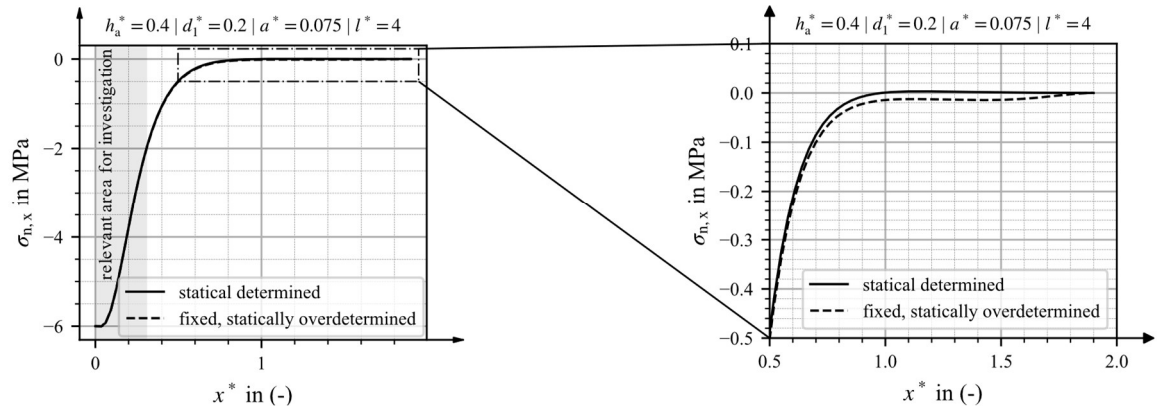

Figure 6: Influence of boundary conditions on the curve of the normal stress in and along x-direction: overview (left) and enlarged section (right)

4.5 Influence of material parameters

To prove the independence of the effective range from the material parameters, a parameter study was carried out with different Poisson ratios and Young's moduli. The parameter range is shown in Table 1.

Table 1: Material parameters for parameter variation

Parameter	Symbol	Min. value	Max. value	Step size	Unit
Young's modulus	E	10	220	10	GPa
Poisson's ratio	ν	0.06	0.48	0.06	-

An influence cannot be determined (Figure 7). The value of the distance from the pressurized surface $x_{\sigma}{}^{*}{}_{\mathrm{n\,x\,0.5p}}$ is constant for all Young's moduli and Poisson's ratios.

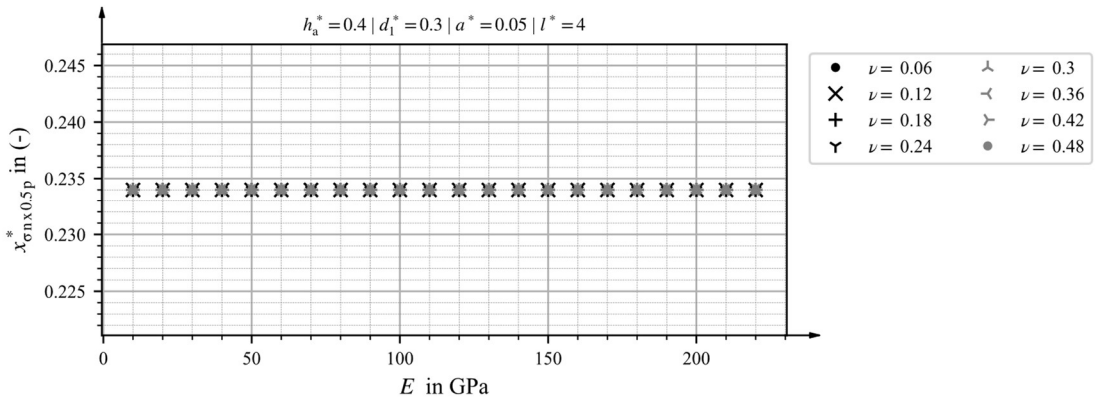

Figure 7: Distance $x_{\sigma n}{}^{*}{}_{\mathrm{x\,0.5p}}$ as a function of Young's modulus and for different Poisson ratios.

4.6 Influence of geometric parameters

The influence of the geometric sizes of the force application area is investigated by varying $d_1{}^{*}$, $h_a{}^{*}$, and a^{*}. An increase in the distance of the force applying surfaces $d_1{}^{*}$ is beneficial for the effective range (Figure 8). The dependence on the distance of the force application surfaces is low. A value of $d_1{}^{*} = 0.2$ is chosen for further investigations. This is considered the lowest distance between the surfaces.

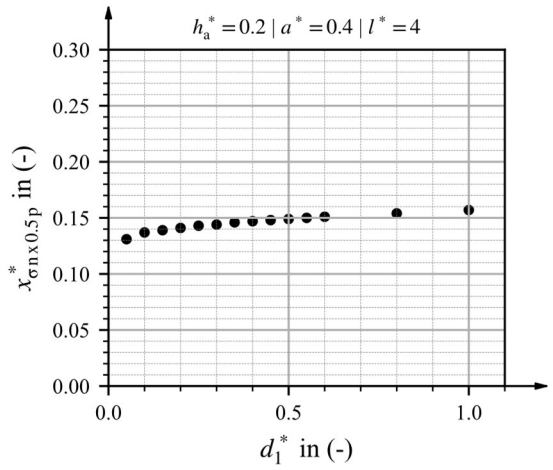

Figure 8: Distance $x_{\sigma n}{}^{*}{}_{\mathrm{x\,0.5p}}$ for different distances between the force-applying surfaces $d_1{}^{*}$

The values for a parameter variation of the actuator height h_a^* and the concrete cover a^* are shown in Table 2. To ensure that the force application area is above the neutral fiber and a positive active moment is generated, the sum of h_a^* and a^* must be less than or equal to 0.5.

Table 2: Range of parameters for geometric variations in 2D

Parameter	Symbol	Min. value	Max. value	Step Size	Unit
actuator height	h_a^*	0.05	0.5	0.025	-
concrete cover	a^*	0.025	0.5	0.025	-

Figure 9 compares $x_{\sigma n\ x\ 0.5p}^*$, h_a^*, and a^*. The effective range rises with increasing height of the pressurized surface h_a^* and increasing concrete cover a^*. From the depiction of the dependence of $x_{\sigma n\ x\ 0.5p}^*$ for different actuator heights, it can be observed that the size a^* only has an influence as long as $a^* < h_a^*$. Above this, $x_{\sigma n\ x\ 0.5p}^*$ increases quasi-linearly with h_a^*. In the range of influence of a^*, an exponential behavior can be observed. The effect of increasing the concrete cover a^* is evident, especially for values of h_a^* greater than 0.2.

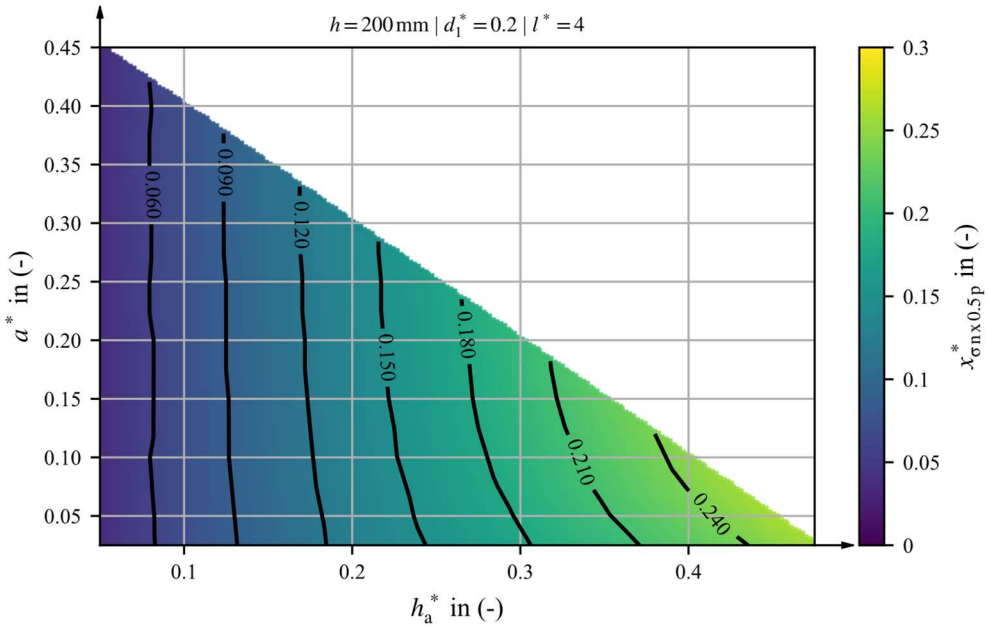

Figure 9: Distance $x_{\sigma n\ x\ 0.5p}^*$ for different h_a^* and a^*

According to this, placing the actuator near the neutral fiber leads to a higher effective range, especially for large heights of the force application areas. This can be used to select the optimum height or edge distance or to determine whether the influence may be negligible. Eventually, a suitable placing distance between the actuators can be selected after choosing the shape of the force-applying surface.

5 ANALYTICAL APPROACH

An equation with the following form appears promising based on the considerations in section 4.6:

$$x^*_{\sigma n\,x\,Xp} = h^*_a \cdot \left(c_1 - c_2 \cdot \langle c_3 - \frac{a^*}{h^*_a}\rangle^3\right) + c_4$$
$$\text{with } \langle c_3 - \frac{a^*}{h^*_a}\rangle = \begin{cases} 0, \ if\ c_3 - \frac{a^*}{h^*_a} \leq 0 \\ c_3 - \frac{a^*}{h^*_a}, if\ c_3 - \frac{a^*}{h^*_a} > 0 \end{cases} \quad (1)$$

An analytical approximation that describes the position of $x^*_{\sigma n\,x,\,0.5p}$ with an average deviation of less than five percent is achieved with $c_1 = 0.65$, $c_2 = 0.12$, $c_3 = 1$, and $c_4 = 0.0075$ mm. Thus follows:

$$x^*_{\sigma n\,x\,0.5p} = h^*_a \cdot \left(0.65 - 0.12 \cdot \langle 1 - \frac{a^*}{h^*_a}\rangle^3\right) + 0.0075\ \text{mm} \quad (2)$$

Figure 10 compares the simulation values and the analytical solution with the factors defined above. The analytical and numerical results match with good quality. Slightly larger deviations occur only in the range of very small concrete covers of a^* below 0.05, which does not appear to be practical.

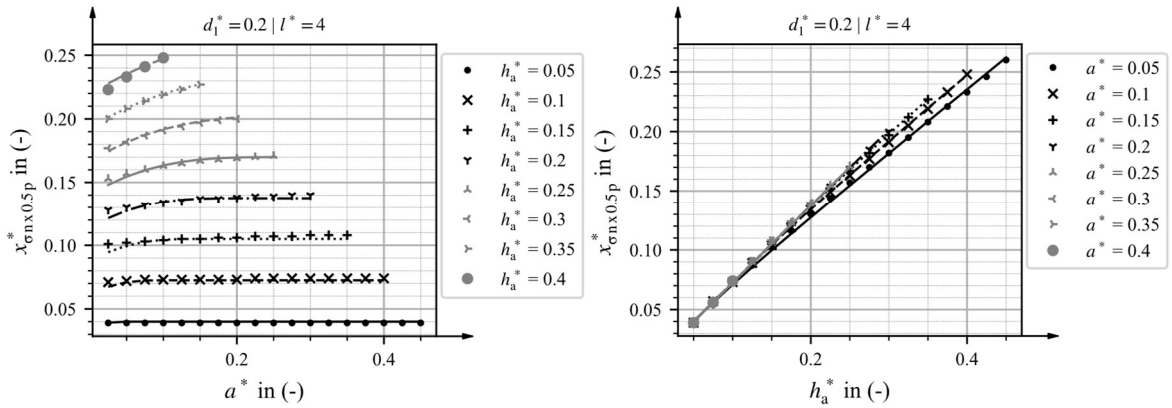

Figure 10: Comparison of the simulated values (dots) and the analytical approximation (lines) for $x^*_{\sigma n\,x\,0.5p}$ as a function of a^* and h_a^*

6 CONCLUSIONS

The integration of actuators into the cross-section of structural elements is an approach to reduce their deflections subjected to bending stress. As a result, the material is utilized more uniformly, which leads to an increased load-bearing capacity. Knowledge of the influence of different parameters on force propagation is essential for the efficient placement of actuators and the optimal rough design of the force application areas. In this paper, the influence of the force application areas of an integrated actuator on the surrounding structure was investigated by performing 2D FE analyses.

By reaching a maximum value of the first principle stress between two actuators, it is assumed that the largest possible upward bending moment is generated. This coincides with an almost uniform normal stress distribution between two actuators. The normal stress does not drop below 80 % of the applied pressure. By analyzing a single actuator, the necessary distance between two actuators was determined. The distance corresponds to twice the distance between a single actuator and the point where the normal stress is 50 % to the pressure applied by the actuator. Various parameters were investigated for their respective influence on the position of this point. Based on this, an analytical approach was determined that describes the effective influence range of the actuator. The size of the effective range of the actuator rises with increasing height of the force application surface and with increasing distance between the actuator and component surface (concrete cover). To actuate a section of a structural element, a few large actuators are consequently more effective than many small ones.

The next step is to extend the study with a three-dimensional model. Here, the influence of the actuator width has to be evaluated. In addition, an analytical approach will be defined that describes the exact pressure propagation. This will provide a more accurate estimate of the distances between the actuators integrated into the structure. If bending deformations of the structural element are to be compensated, which is the primary objective, the actuators should be positioned as far eccentrically as possible from the neutral plane. This fact is in contrast to the results of this study, where the force propagation increases with the material cover. Therefore, further investigation is needed to achieve the overall goal of precise actuation with as few actuators as possible.

ACKNOWLEDGMENTS

This work is funded by the Deutsche Forschungsgemeinschaft (DFG, German Research Foundation) – Project-ID 279064222 – SFB 1244. The authors are grateful for the generous support.

REFERENCES

[1] Scrivener, K.; John, V. and Gartner, E. Eco-efficient cements: Potential economically viable solutions for a low-CO_2 cement-based materials industry, *Cement and Concrete Research*. 2018.

[2] Sobek, W. Ultra-lightweight construction. *International Journal of Space Structures*, Vol. 31, pp. 74-80, 2016.

[3] Kelleter, C. et al. Adaptive Concrete Beams Equipped with Integrated Fluidic Actuators, *Frontiers in Built Environment* 6, 2020.

[4] Burghardt, T. et al. Investigations of a Large-Scale Adaptive Concrete Beam with Integrated Fluidic Actuators. *Civil Engineering Design, 2022.*

[5] Soong, T. T. *Active Structural Control: Theory and Practice*. Wiley; Longman Scientific & Technical, New York, Harlow, Essex, 1990. ISBN 0-582-01782-3.

[6] Senatore, G. et al. *Shape control and whole-life energy assessment of an 'infinitely stiff' prototype adaptive structure*. Smart Mater. Struct. 27, 2018, 1.

[7] Blandini, L. et al. Der Demonstrator D1244: das weltweit erste adaptive Hochhaus. *Bautechnik*, 2022, https://doi.org/10.1002/bate.202100065.
[8] Teuffel, P. *Entwerfen adaptiver Strukturen.* Institut für Leichtbau Entwerfen und Konstruieren, Universität Stuttgart. 2004. Dissertation.
[9] Neuhaeuser, S. et al. Stuttgart SmartShell – A Full Scale Prototype of an Adaptive Shell Structure. Institut für Leichtbau Entwerfen und Konstruieren, Universität Stuttgart. *Journal of the International Association for Shell and Spatial Structures*, 2013. Dissertation.
[10] Schnellenbach-Held, M. et al. Adaptive Spannbetonstruktur mit lernfähigem Fuzzy-Regelungssystem. *Berichte der Bundesanstalt für Strassenwesen B, Brücken- und Ingenieurbau*. 2014, Bd. 101
[11] Sobek, W. et al. Adaptive Hüllen und Strukturen. *Bautechnik*. 98, 2021, 3, pp. 208-211.
[12] Kelleter, C. et al. Actuation concepts for structural concrete elements under bending stresses. *European Conf. on Computational Mechanics (ECCM) and 7th European Conf. on Computational Fluid Dynamics (ECFD).* 2018.
[13] Kelleter, C. et al. Actuation of structural concrete elements under bending stress with integrated fluidic actuators. *Int. Conf. on Structural Engineering, Mechanics and Computation (SEMC)*. 2019.
[14] Mises, R. V. *On Saint Venant's principle*. Bull. Amer. Math. Soc. 51, pp. 555–563, 1945.